

Advances in Photoacoustic Imaging Reconstruction and Quantitative Analysis for Biomedical Applications

Lei Wang, Weiming Zeng*, Kai Long, Hongyu Chen, Rongfeng Lan, Li Liu, Wai Ting Siok, Nizhuan Wang*

Abstract—Photoacoustic imaging (PAI) represents an innovative biomedical imaging modality that synergistically integrates the high spatial resolution of optical imaging with the deep penetration capabilities of acoustic waves, while maintaining enhanced safety. Despite its significant potential for both preclinical and clinical applications, the clinical adoption of PAI is hindered by critical challenges, including the inherent trade-offs between penetration depth and spatial resolution, as well as the need for faster imaging speeds. This review provides an in-depth exploration of the foundational principles of PAI, with a particular emphasis on its three primary implementations: photoacoustic computed tomography (PACT), photoacoustic microscopy (PAM), and photoacoustic endoscopy (PAE). A critical evaluation of their respective strengths and practical limitations is presented. Additionally, the paper highlights recent advancements in image reconstruction and artifact mitigation, leveraging both conventional and deep learning (DL) methodologies across PACT, PAM, and PAE, showcasing their potential to significantly enhance image quality and accelerate imaging processes. Furthermore, the review examines recent progress in quantitative PAI, including the accurate quantification of hemoglobin concentration, oxygen saturation, and other critical physiological parameters within tissues. Finally, the discussion outlines current trends and future research directions in PAI, underscoring the transformative role of deep learning in driving the continued evolution and clinical translation of this field.

Index Terms—Photoacoustic imaging, Deep learning, Photoacoustic Image Reconstruction, Quantitative Analysis

I. INTRODUCTION

A. Fundamentals of Photoacoustic Imaging

Optical and ultrasound imaging are well-established and advanced techniques that have become essential in medical imaging [1]. Optical imaging is valued for its high sensitivity and contrast but is limited by light diffusion in biological tissues, which restricts high-resolution imaging at deeper levels [2]. Conversely, ultrasound imaging (USI) is widely used and

advantageous for its low scattering and deep tissue penetration, particularly in cardiovascular, abdominal, and digestive imaging [3], [4]. However, low-contrast images result from minimal differences in acoustic-physical properties among tissues, and the absence of microbubbles as contrast agents limits fine structural visualization. Therefore, a novel imaging approach is needed to achieve high spatial resolution while overcoming depth challenges [5]. Such technologies could merge the high contrast of optical imaging with the deep penetration of ultrasound, enhancing diagnosis and treatment monitoring in clinical settings [6], [7].

PAI utilizes the photoacoustic effect, integrating optics and acoustics, and holds significant potential for diverse applications [7], [8]. It involves directing short-pulsed light at biological tissues, where absorption varies with wavelength. Endogenous chromophores, such as DNA, RNA, hemoglobin, melanin, collagen, and lipids, along with FDA-approved contrast agents like indocyanine green (ICG) and methylene blue, absorb the light. This absorption causes a rapid temperature increase, leading to thermal expansion and ultrasound wave generation. The waves' origin is determined by their time-of-flight, providing insights into the tissue's optical absorption properties. An ultrasound transducer (USTR) detects these signals, which are processed to create 2D or 3D images. The PAI process includes pulsed laser emission, light absorption, thermal expansion, ultrasonic wave generation, detection, and image reconstruction. As shown in Fig. 1, the PAI process involves pulsed laser emission, light absorption, thermal expansion, ultrasonic wave generation, detection, and image reconstruction.

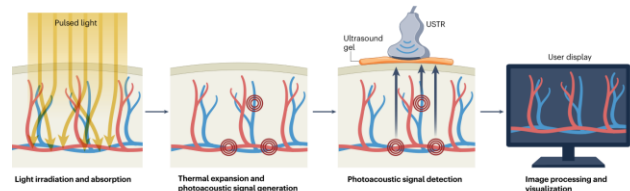


Fig. 1. The Complete Procedure of PAI [7].

This work was supported in part by the Hong Kong Polytechnic University Start-up Fund (Project ID: P0053210) and in part by Hong Kong RGC GRF under Grant 14220622 and Grant 14204321.

Lei Wang Weiming Zeng and Hongyu Chen are with the Laboratory of Digital Image and Intelligent Computation, Shanghai Maritime University, Shanghai, China. Lei Wang is also with the School of Electronic Engineering and Intelligent Manufacturing, Anqing Normal University, Anqing, China.

Kai Long and Li Liu are with School of Engineering, Great Bay University and Dongguan Great Bay Institute for Advanced Study, Dongguan, China.

Rongfeng Lan is with the Department of Cell Biology & Medical Genetics, School of Basic Medical Sciences, Shenzhen University Medical School, Shenzhen, China.

Wai Ting Siok and Nizhuan Wang are with the Department of Chinese and Bilingual Studies, The Hong Kong Polytechnic University, Hong Kong SAR, China. (*correspondence e-mail: wangnizhuan1120@gmail.com or zengwm86@163.com).

image reconstruction [7], [9].

Specifically, the stress relaxation time denotes the time required for the stress (pressure) to dissipate from the heated volume [7]. When the laser pulse duration is shorter than the stress relaxation time, stress confinement is indicated; when thermal confinement is also realized, the fractional volume expansion ($\Delta V/V$) is negligible [10], as long as the following conditions are satisfied:

$$\frac{\Delta V}{V} = -\kappa \Delta p + \beta \Delta T = 0, \quad (1)$$

where Δp and ΔT represent the pressure and temperature change respectively; κ represents isothermal compressibility, and β denotes the thermal coefficient of volume expansion. Further, the initial local pressure rise (p_0) after laser excitation can be calculated as:

$$p_0 = \frac{\beta}{\kappa \rho C_v} \eta_{th} \mu_a F = \Gamma \eta_{th} \mu_a F = \Gamma E_a, \quad (2)$$

where ρ denotes the mass density, C_v is the specific heat capacity at a constant volume, η_{th} is the percentage of specific optical absorption that is converted to heat, μ_a is the optical absorption coefficient, F is the optical fluence, and E_a is the absorbed optical energy. Thus, the initial local pressure rise is directly proportional to the non-radiative optical energy absorption via the proportionality factor Γ , known as the Grüneisen coefficient.

B. Advances of PAI

Biomedical imaging techniques, such as computed tomography (CT), magnetic resonance imaging (MRI), positron emission tomography (PET), optical imaging (OI), and ultrasound imaging (USI) [6], are crucial in medicine. They provide essential anatomical and physiological insights for disease diagnosis, treatment planning, and early health risk detection [11]. However, these techniques have limitations, including issues with diagnostic specificity, imaging speed, patient exposure to ionizing radiation, and dependence on contrast agents.

PAI overcomes the depth limitations of traditional OI, which is restricted by light diffraction to depths of less than 1 mm [12]. By integrating optical imaging's high sensitivity with ultrasound's deep penetration, PAI offers high resolution, rapid imaging, and greater depth [13]. Enabling high-contrast visualization of deeper tissues, PAI is valuable for studying the morphological, physiological, pathological, and metabolic characteristics of tissues [14]. Choosing the right contrast agent is crucial for enhancing image specificity in PAI. Exogenous agents offer high sensitivity and molecular targeting, whereas endogenous agents like hemoglobin, lipids, melanin, and water are preferred for non-invasive imaging due to their natural

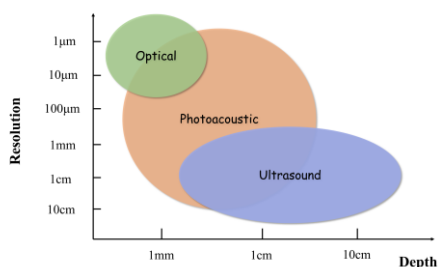


Fig. 2. Resolution and depth characteristics in photoacoustic, ultrasonic, and optical imaging.

presence and non-toxicity [15]. Higher ultrasound frequency and bandwidth enhance spatial resolution but reduce imaging depth [16].

Despite challenges such as acoustic attenuation, coupling stability, bandwidth limitations, and electromagnetic interference, PAI stands out for its non-invasiveness, lack of ionizing radiation, high contrast, and high spatial resolution, offering significant potential in biomedical research [17]. The sensitivity and resolution of PAI depend on factors such as tissue optical absorption contrast, laser pulse duration, and image reconstruction algorithm precision [18]. Thus, developing high-quality image reconstruction algorithms is crucial for ensuring PAI imaging quality. Since its first successful use in imaging live mouse brains in the early 21st century, PAI has significantly advanced in device development, algorithm optimization, and functional imaging [19]. Table 1 compares various imaging modalities [20].

Table 1 highlights that PAI effectively overcomes the limitations of optical coherence tomography (OCT) and USI, particularly the absence of speckle artifacts. By leveraging the photoacoustic effect, PAI enhances tissue contrast and integrates ultrasonic detection, enabling high-resolution imaging. Furthermore, it reconstructs optical absorption and attenuation coefficient distributions, facilitating quantification of blood oxygen saturation levels [21]. Figure 2 illustrates the resolution and depth characteristics of various imaging modalities, including ultrasound, optical, and photoacoustic imaging. In conclusion, PAI demonstrates significant potential in biomedical research and clinical applications, offering high-contrast, high-resolution imaging with deep-tissue measurement capabilities.

II. KEY IMPLEMENTATIONS OF PAI

Advancements in laser technology from the late 1970s to early 1980s spurred studies on the photoacoustic effect, laying the foundation for the development of PAI [21]. By the early 21st century, techniques such as PACT, PAM, and PAE had matured, significantly advancing PAI and expanding its biomedical applications, thus opening new research and clinical avenues [22], [23], [24]. Figure 3 illustrates the three main methodologies employed in PAI [25].

A. PACT

PACT is one of the earliest developed imaging techniques, providing a radiation-free and safe approach for human imaging [26], [27]. It has the potential to expand the imaging field of view and enhance penetration, benefiting various biomedical applications, such as quantitative analysis of blood oxygen saturation (sO_2) in cancer diagnosis [14], [28].

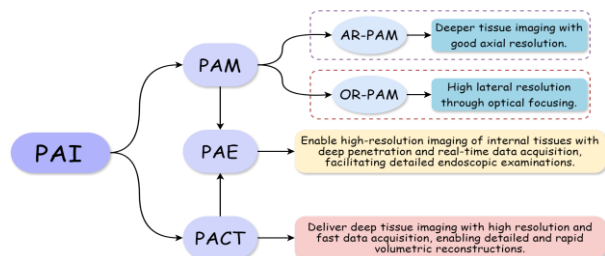


Fig. 3. Three Key Implementations of PAI.

PACT employs a wide-diameter, non-focused pulsed laser beam to illuminate tissue surfaces, with a non-focused ultrasonic detector array capturing the photoacoustic signals [22]. Inversion algorithms process these signals to reconstruct the initial acoustic field, producing high-resolution images from cellular to organ levels, with detail down to hundreds of micrometers [29], [30]. PACT offers moderate spatial resolution, significant penetration depth, and fast imaging speeds. The choice of ultrasonic transducer array depends on the application: linear arrays suit small animals or surface tissues, while hemispherical arrays are better for broader human imaging, particularly for breast cancer detection [31], [32]. PACT's role in breast cancer detection has driven advances in clinical research, with multiple systems in development [33]. While effective for deep imaging, PACT has relatively moderate resolution [34], and contrast mechanisms vary between macroscopic and microscopic imaging [17]. Table 2 summarizes its advantages and constraints.

Researchers have advanced PACT through innovations in imaging devices, contrast agents, and models [35]. PACT employs reconstruction algorithms to convert photoacoustic signals into acoustic source distributions, creating images [36]. These algorithms are critical for imaging precision [37]. However, challenges such as sparse angular views and limited bandwidth can reduce image quality [36], [38]. The reconstruction process involves an acoustic inverse problem with incomplete data. To enhance PACT in biomedical imaging, optimizing current technologies and developing new strategies are necessary [39].

TABLE 1. COMPARATIVE ANALYSIS OF VARIOUS IMAGING MODALITIES.

Characteristics	OCT	US	PAI
Depth	1mm	60mm	8cm
Contrast	Good	Poor	Excellent
Resolution	Excellent (0.01mm)	Excellent (0.3mm)	Excellent
Scattering	Significant	Minimal	Mixed
Speckle	Present	Present	None

Note: OCT - Optical Coherence Tomography; US - Ultrasound Imaging; PAI - Photoacoustic Imaging.

B. PAM

PAM has become essential for microscopic imaging over the past decade, leveraging its unique optical absorption contrast mechanism [27], [30]. As a versatile biomedical tool, it enables structural, functional, and molecular imaging using both endogenous and exogenous contrast agents. Applications include blood flow perfusion, oxygenation imaging, tumor imaging, and brain imaging, with hemoglobin serving as an endogenous absorber [38], [40]. Compared to PACT's

TABLE 2. ADVANTAGES AND CONSTRAINTS OF THE PACT MODALITY.

Modality	Advantages	Constraints
PACT	Radiation-free and safe; Wide field of view; Non-invasiveness; Greater imaging depth; Fast imaging speed; Moderate spatial resolution; Versatile for cellular to organ-level imaging.	Trade-off challenge between cost and SNR; Less prominent resolution; Differences in macro-micro contrast.

TABLE 3. ADVANTAGES AND CONSTRAINTS OF THE PAM MODALITY.

Characteristics	OR-PAM	AR-PAM
Advantages		
Lateral Resolution	High (<5 μm); Determined by ultrasound transducer bandwidth;	Moderate (>50 μm); Determined by ultrasound transducer bandwidth;
Axial Resolution	Limited (~1-2 mm); Strong optical focusing enhances contrast.	Deeper (~3-10 mm); Applicable for broader imaging applications.
Depth Penetration	Suitable for high-precision surface imaging.	Suitable for deeper tissue imaging.
Contrast Mechanism		
Imaging Precision		
Constraints		
Depth Penetration	Restricted by light scattering effects;	Constrained by reduced lateral resolution and elevated background noise;
Lateral Resolution	Limited applicability for deep tissue imaging;	Inferior resolution compared to OR-PAM;
Imaging Speed	Speed constrained by mechanical scanning;	Slower due to broader imaging coverage;
Contrast Noise Ratio	Challenged by reduced contrast in deeper tissues;	Higher background noise impacting clarity;
Clinical Application	Constrained by depth and speed limitations.	Challenged by lower resolution and noise in deeper tissues.

centimeter-level penetration depth, PAM offers superior resolution at similar depths [18], [33]. PAM uses focused short-pulse laser illumination and collects photoacoustic signals at discrete points with a focused ultrasound transducer. The data acquisition system amplifies and samples these signals, progressively forming the image through point-by-point scanning without additional inversion algorithms, making it highly valuable for biomedical applications. By overcoming light scattering, PAM surpasses the depth limitations of high-resolution optical imaging, achieving deep tissue imaging with high precision, particularly for skin and tissue surfaces at the micron level [31].

PAM is categorized into optical-resolution PAM (OR-PAM) and acoustic-resolution PAM (AR-PAM) based on the relative sizes of optical and acoustic beam focuses [5], [18], [25]. OR-PAM uses a tightly focused light source, achieving high lateral resolution (<5 μm), but is limited to a penetration depth of 1-2 mm due to light scattering. In contrast, AR-PAM employs weakly focused or collimated light beams, enabling deeper imaging (3-10 mm) with lateral resolution determined by the acoustic focal spot (>50 μm), though with more background noise. Both types have axial resolution dependent on the ultrasound transducer's bandwidth. A key challenge is achieving high lateral resolution in AR-PAM without compromising imaging depth. Most OR-PAM systems use mechanical scanning for optical excitation and ultrasound detection, limiting imaging speed. Nonetheless, OR-PAM is valuable in biomedical research, such as tumor angiography and melanoma cell imaging [31], [41]. AR-PAM excels in deep tissue imaging beyond 1 mm, overcoming light diffusion limitations, and can measure various biomedical parameters,

including oxygenated and deoxygenated hemoglobin concentrations, blood flow velocity, and oxygen metabolism rates [20].

A key technical challenge for PAM is balancing spatial resolution and imaging speed [41], [42]. Clinical adoption of PAM has been hindered by factors such as high laser excitation doses, limited imaging speeds, and suboptimal image quality [17], [31]. These parameters are interdependent, and current efforts focus on developing advanced image and signal processing models to improve image quality [43]. Table 3 summarizes the advantages and constraints of PAM.

C. PAE

The applicability of traditional PACT and PAM is limited for imaging internal tissues and organs, such as the digestive system and vascular walls. To overcome this limitation, researchers have integrated non-invasive photoacoustic tomography with endoscopic technology, enabling imaging of deep internal tissue structures [19], [44]. Although PAE is the most recent PAI technique, it has developed rapidly and can image internal tissues such as the digestive tract, blood vessels, and the urogenital system, thus becoming a significant area of research [44].

PAE is well-suited for detecting lesions in biological cavities such as the nasal cavity, digestive tract, and arterial vessels, providing high-quality images of superficial tissues for diagnostic purposes. It utilizes miniaturized MEMS scanning devices and fiber optic sensors to reduce system size, facilitating in vivo imaging for examining organ conditions or lesions. However, spatial constraints within the lumen limit the detector's angular range for collecting photoacoustic signals, potentially affecting image quality. Table 4 summarizes the advantages and constraints of PAE, and Table 5 compares the characteristics of the three principal PAI modalities.

The following sections will discuss image reconstruction techniques for PAI, including conventional and deep learning methods, and present a quantitative analysis of PAI, as illustrated in Fig. 4.

III. CONVENTIONAL RECONSTRUCTION IN PAI

The core principle of PAI is to map the distribution of the optical absorption coefficient within tissues, which directly correlates with the initial acoustic pressure distribution. Developing robust reconstruction models is essential for accurately reconstructing the initial acoustic pressure from the acquired photoacoustic signals [45].

Conventional reconstruction methods can be broadly classified into analytical and iterative methods (shown in Fig. 5) [46]. Analytical reconstruction methods use time and

TABLE 4. ADVANTAGES AND CONSTRAINTS OF THE PAE MODALITY.

Characteristics	Advantages	Limitations
PAE	Non-invasive; Suitable for internal imaging; High-quality imaging of shallow tissue; Miniaturized system for in vivo use; Aids in lesion detection and diagnosis.	Limited spatial resolution; Restricted field of view; Susceptibility to noise; Interference from background tissues; Signal attenuation.

TABLE 5. CHARACTERISTIC COMPARISON OF THREE MODALITIES OF PAI.

Modalities	Resolution	Field of View	Depth	Cost
PACT	Low	Large	Deep	Expensive
AR-PAM	High	Limited by scanning range	Moderate	General
OR-PAM	High	Small	Shallow	Expensive
PAE	High	Small	Shallow	General

TABLE 6. A BRIEF SUMMARY OF DL-BASED RECONSTRUCTION APPROACHES FOR PACT.

DL methods	Models	Backbones
DL-based reconstruction During Pre-processing Stage	FC-DNN [66]	This study proposed a fully connected deep neural network (FC-DNN) to correct sonograms acquired by each transducer channel, broadening the bandwidth of received data and increasing the SNR of beamformed images.
DL-based reconstruction Within Direct-processing Stage	Res-Unet [69]	This study proposed a model that uses the entire raw signals as inputs with learned weights/filters to mitigate image reconstruction ill-posedness, and the Res-Unet successfully generated high-quality images with sharp edges and reduced artifacts
DL-based reconstruction Throughout Post-processing Stage	FD-UNet [70]	This study used the Fully Dense U-Net (FD-UNet) for post-processing reconstruction images, enhancing inter-layer feature information transmission and reducing redundant feature learning.
	PA-GAN [73]	This study removed artifacts due to limited view data using an unsupervised learning approach.
	PAT-AND [74]	This study designed an unsupervised learning Artifacts Disentangling Network (ADN) to address artifact issues in extremely sparse view scenarios.
	MDAEP [75]	This study combined Multi-Channel Denoising AutoEncoder Prior (MDAEP) with model iterations for high-resolution accelerated sparse reconstruction, integrating PAT's physical model with unsupervised multi-channel deep learning networks.
	DuDounet [71]	This study shared nearly identical texture information across dual domains but distinct artifact information, teaching the network how to differentiate these at the input level.
	NA Mechanism for Sparse PACT Reconstruction [77]	This study proposed a novel solution that employed the neighborhood attention (NA) mechanism for sparse PACT.

frequency domain techniques to find optimal solutions, such as time reversal (TR) [47], [48], delay-and-sum (DAS) [49], [50]

in the time domain, and filtered back projection (FBP) [51] in the frequency domain.

High-fidelity image reconstruction is crucial for improving the accuracy of photoacoustic imaging, as it converts raw signals from ultrasonic transducers into images of initial pressure distributions [52]. When data acquisition is incomplete, conventional PAI imaging reconstruction methods such as back-projection [53], TR, and DAS may result in diminished image quality and reduced imaging depth [54].

Unlike analytical methods, iterative reconstruction employs optimization and regularization to solve equations, offering higher signal-to-noise ratios (SNR) and improved image quality but requiring more computational power. It assumes ideal conditions such as high sampling rates and uniform sound speed, which are often not met in real scenarios, leading to errors and degraded image quality. While iterative methods can partially mitigate these issues, they demand substantial computational resources and careful selection of regularization techniques [55].

Despite significant engineering efforts to address PAI's technical challenges, most solutions rely on complex, expensive hardware and time-consuming image reconstruction processes,

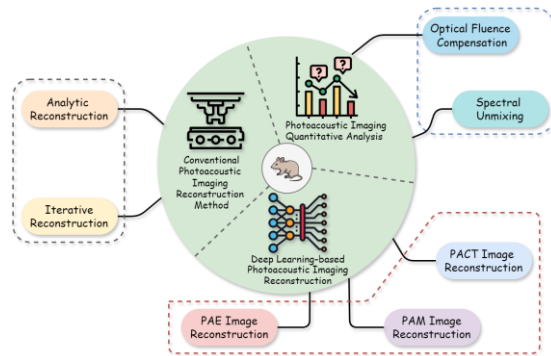


Fig. 4. Illustrative overview outlining the scope of this review.

including iterative methods. These approaches often require balancing parameters like speed vs. field of view and resolution vs. penetration depth. Consequently, PAI urgently needs innovative solutions to address these challenges with a fresh perspective [56].

IV. DEEP LEARNING-BASED RECONSTRUCTION IN PAI

Deep learning has rapidly advanced, driven by large datasets and powerful computing resources, and is now crucial for tasks including image classification, segmentation, reconstruction, super-resolution, and disease prediction. In PAI reconstruction, it surpasses traditional algorithms by generating high-quality

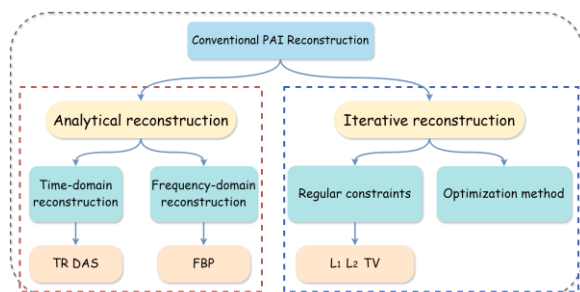


Fig. 5. Illustration of conventional PAI reconstruction methods.

images with enhanced SNR, even at low pulse energy levels [57]. Its integration into PAI significantly improves artifact removal, denoising, and super-resolution [32], [51], [54], and enhances image quality under non-ideal conditions, addressing challenges such as sparse sampling, limited views, restricted bandwidth, heterogeneous media, finite aperture sizes, and insufficient laser power.

Antholzer *et al.* [59] introduced CNNs for PAI reconstruction in 2017, enhancing reconstruction speed and image quality by learning complex mappings and optimal features. In PACT, DL models yield high-fidelity 3D images [60]; in PAM, they enable high-contrast, high-resolution imaging of biological tissues [20]; and in PAE, they improve clarity and detail by learning rich features from limited datasets [13].

1) PACT Image Reconstruction

PACT is an emerging imaging technique that reconstructs initial pressure distributions from acoustic signals for high-contrast deep tissue visualization [36]. A key challenge is achieving high SNR images with cost-effective equipment. Sparse sampling often results in poor reconstructions with artifacts [39], [42]. Deep learning methods have been developed and applied in PACT to enhance image reconstruction quality, as shown in Table 6 [61], [49], [50], [64], [65]. Figure 6 illustrates the integration of acoustic inversion and deep learning in processing Radio Frequency (RF) data for image reconstruction, highlighting pre-processing, post-processing, and direct processing approaches [10].

(1) DL-based reconstruction During Pre-processing Stage

Data preprocessing employs neural networks to optimize raw data for reconstruction, addressing limitations such as insufficient bandwidth or limited-angle data. Specific networks process photoacoustic sinograms, enhancing signal bandwidth and resolution. Gutta *et al.* [66] utilized a fully connected deep neural network (FC-DNN) to correct sonograms, broadening the effective bandwidth and increasing the SNR of beamformed images by approximately 6 dB. Similar approaches have been reported by other researchers [67], [68].

(2) DL-based reconstruction Within Direct-processing Stage

Direct processing in neural networks for photoacoustic imaging involves using architectures that map incoming photoacoustic signals directly to resulting images, bypassing traditional step-by-step processing. Feng *et al.* [69] introduced an end-to-end Res-Unet model, combining ResNet and Unet architectures, to generate high-quality PA-images from raw sensor inputs. The model features skip connections and a residual learning mechanism, which enhance training efficiency and prevent network degradation. This approach produces images with clear edges and fewer artifacts, simplifying the imaging pipeline and potentially reducing computational requirements. Comparisons with traditional methods and other deep learning models could provide further insights into its performance and practical implications. This advancement holds promise for enhancing photoacoustic imaging in biomedical applications.

(3) DL-based reconstruction Throughout Post-processing Stage

Post-processing techniques enhance images from conventional algorithms, particularly addressing challenges

from sparse sampling and limited-angle acquisitions in photoacoustic imaging. Antholzer *et al.* [59] used a U-Net network to refine FBP-reconstructed images under limited-angle conditions. Guan *et al.* [70] developed Fully Dense U-Net (FD-UNet) with dense connections for improved feature transmission. Zhang *et al.* [71] introduced Dual Domain Unet (DuDoUnet) with an Information Sharing Block to reduce artifacts. Lan *et al.*'s [72] JEFF-Net employs a DL fusion framework to suppress artifacts, while unsupervised methods like PA-GAN [73] and PAT-AND [74] address data labeling issues, with PAT-AND performing well under sparse angular conditions.

Physics-informed DL approaches integrate physical models with neural networks. Song *et al.* [75] proposed a fast sparse reconstruction strategy combining a multi-channel denoising autoencoder prior with model-based iteration. Guo *et al.* [76] introduced a high-quality PACT strategy under limited-angle conditions using a fractional diffusion model, enhancing imaging quality and speed.

Sparse sampling is crucial for rapid data acquisition in PAI, but reconstructing high-quality images from sparse data is challenging. Chan *et al.* [77] proposed a neighborhood attention mechanism for sparse PACT reconstruction, emphasizing local neighborhood information. Tong *et al.* [78] developed the Feature Projection Network (FPNet) for direct reconstruction from sparse and limited-angle data, though it requires significant computational resources.

(4) DL-based reconstruction in the Hybrid-processing Stage

Lan *et al.*'s Y-Net was a hybrid DL framework that combines direct reconstruction with postprocessing to extract information from raw data and preliminary reconstructed images [79]. Inspired by the U-Net network, Y-Net reconstructs the initial PA pressure distribution by optimizing both raw data and beamformed images using two encoder paths and one decoder path.

2) PAM Image Reconstruction

In PACT and PAM, DL is applied differently. In PAM, without requiring inverse reconstruction, DL models directly map input signals to output images, enhancing image quality [3], [59]. This approach is effective for addressing challenges in PAM, such as improving reconstructions, removing artifacts, denoising data, enhancing spatial resolution, and up-sampling sparse data. Additionally, DL efficiently approximates nonlinear spatial mappings with GPU acceleration. Existing reconstruction algorithms have been continuously refined. This section examines the impact of current DL models on photoacoustic image performance in PAM, focusing on resolution, noise reduction, and imaging depth.

(1) Deep Learning for Resolution Enhancement in PAM Reconstruction

Spatial resolution is crucial for evaluating photoacoustic images, influenced by both hardware and reconstruction algorithms. Reducing spatial sampling density and increasing scanning step size in PAM to speed up imaging degrades resolution and causes aliasing. Deep learning has been applied to lower laser pulse energy and enhance undersampling in PAM.

Recently, a non-pretrained Deep Iterative Prior (DIP) model was developed to enhance undersampled PAM images and speed up imaging [80]. This model iteratively optimizes fully

sampled images from undersampled data using a known downsampling mask, enhancing generalization without paired training. It outperformed interpolation methods and pretrained DL models on mouse brain vasculature and bio-printed gel images without prior training data, marking its first application in PAM.

Seong *et al.* [81] developed a DL-based method for 3D volumetric reconstruction in PAM, reducing imaging time and data volume by fully reconstructing undersampled datasets. They adapted SRResNet and validated its performance, achieving the first DL-based 3D reconstruction of undersampled PAM data.

Li *et al.* [82] introduced PSAD-UNet, a model that enhances transcranial photoacoustic imaging by mitigating bone plate effects, with broad applications in both preclinical and clinical settings. Wang *et al.* [83] developed PADA U-Net, which reconstructs full images from undersampled data, overcoming the trade-off between imaging speed and spatial resolution. Shahid *et al.* [84] proposed BRn-ResNet, which improves U-Net's training stability and reduces artifacts from sparse data through residual blocks, achieving an SSIM of 0.97.

Cao *et al.* [85] proposed a mean-reverting diffusion model for AR-PAM, employing iterative reverse-time SDE to balance imaging depth and lateral resolution, thereby enhancing imaging quality and broadening applicability without sacrificing depth. Le *et al.* [86] implemented a computational strategy with two GANs for semi/unsupervised high-resolution, sensitive reconstruction in AR-PAM, maintaining imaging capability at enhanced depths. Cheng *et al.* [87] utilized deep learning for image transformation to improve deep penetration in OR-PAM.

Zhao *et al.* [88] proposed a multi-task residual dense network (MT-RDN) to enhance image quality in traditional OR-PAM at ultra-low laser doses, incorporating multi-supervision learning, dual-channel acquisition, and densely connected layers for richer reconstruction details.

(2) Deep Learning for Image Denoising in PAM Reconstruction

Noise significantly impacts photoacoustic image reconstruction, causing artifacts. It arises from hardware limitations and phase mismatches due to inhomogeneous sound velocity and tissue scattering. Zhou *et al.* [89] introduced a denoising method combining empirical mode decomposition (EMD) and conditional mutual information, where EMD decomposes noisy signals into intrinsic mode functions (IMFs), and conditional mutual information aids in denoising.

Liu *et al.* [90] developed UPAMNet, a deep learning network that integrates image prior knowledge to enhance super-resolution and denoise photoacoustic microscopy images. By employing three attention-based modules and mixed training constraints, UPAMNet improved PSNR by 0.59 dB and 1.37 dB for 1/4 and 1/16 undersampled images, respectively, and boosted denoising by 3.9 dB.

In photoacoustic imaging, spatial resolution is degraded by factors such as ultrasound attenuation, phase deviations from sound speed variations, and signal waveform broadening. He *et al.* [91] addressed this by proposing an attention-enhanced GAN with an improved U-net generator to remove noise from PAM images.

TABLE 7. DL-BASED RECONSTRUCTION APPROACHES FOR PAM.

Aims	Models	Backbones
Deep Learning-Driven Resolution Enhancement in PAM Reconstruction	DIP [80]	This study proposed a DIP model that iteratively optimizes a fully sampled image to approximate the undersampled image using a known downsampling mask, enhancing generalization capabilities.
	SRResNet [81]	This study proposed a deep learning-based method to reconstruct undersampled PAM data in 3D, enhancing imaging speed 80-fold and reducing data volume 800-fold, with improvements to the SRResNet framework for better applicability.
	PADA U-Net [83]	This study proposed the Photoacoustic Dense Attention U-Net (PADA U-Net) model to reconstruct fully scanned images from undersampled ones, breaking the trade-off between imaging speed and spatial resolution.
	BRn-ResNet [84]	This study proposed BRn-ResNet to enhance training stability and eliminate subsampling artifacts in photoacoustic imaging, addressing data insufficiency and training interference.
	Mean-reverting diffusion model [85]	This study proposed a novel mean-reverting diffusion model to balance imaging depth and lateral resolution in AR-PAM and OR-PAM, achieving optical-level resolution with deep penetration.
	MT-RDN [88]	This study proposed the Multi-Task Residual Dense Network (MT-RDN), which integrates multi-supervision learning, dual-channel sample acquisition, and rational weight distribution.
Deep Learning for Image Denoising in PAM Reconstruction	UPAMNet [90]	This study proposed UPAMNet, an end-to-end network with attention blocks and multi-level priors, for high-fidelity PAM image super-resolution and denoising.
	PnP Prior [93]	This study proposed a deep CNN-based prior integrated into a model-based reconstruction framework for photoacoustic microscopy, validated through in vivo AR-PAM experiments, using FFDNet for adaptive AWGN denoising, enhancing image contrast, resolution, and detail.
Deep Learning for Imaging Depth Enhancement in PAM Reconstruction	ResUnet-AG [94]	This study proposed a two-stage deep learning strategy for AR-PAM, using a residual U-Net with attention gates to recover high-resolution photoacoustic images at varying depths.
	DiffPam [95]	This study proposes a pre-trained diffusion model for PAM image reconstruction, enabling super-resolution, denoising, and inpainting with simplified training.

The low spatial resolution of AR-PAM imaging has limited its adoption [92]. Previous models lacked flexibility or required complex priors and couldn't adapt to different degradation models. Zhang *et al.* [93] developed a deep CNN-based model that adaptively handles various degradation functions in AR-PAM image enhancement. This model improves PSNR, SSIM, SNR, and CNR in both simulated and in vivo images by learning vascular image statistics as a plug-and-play prior,

TABLE 8. A BRIEF SUMMARY OF DL-BASED RECONSTRUCTION APPROACHES FOR PAE.

Models	Backbones
Focus U-Net [97]	This study incorporated several architectural modifications into the Focus U-Net, including the addition of short-range skip connections and deep supervision.
Wavelet Transform and Guided Filter Decomposition-Based Fusion Approach [98]	This study proposed an approach to improve the visual quality of endoscopic images by using artificially generated sub-images and image fusion techniques.
Contrast Limited Adaptive Histogram Equalization (CLAHE) [99]	This study proposed a method to enhance endoscopic images by generating three complementary sub-images using Contrast Limited Adaptive Histogram Equalization (CLAHE), image brightening, and detail enhancement.
Approximate Gaussian acoustic field [100]	This study proposed a new photoacoustic/ultrasound endoscopic imaging reconstruction algorithm based on the approximate Gaussian acoustic field which significantly improves the resolution and signal-to-noise ratio (SNR) of the out-of-focus region.
Improved back-projection (IBP) algorithm [101]	This study developed an improved back-projection (IBP) algorithm for focused detection over centimeter-scale imaging depth and a deep-learning-based algorithm to remove electrical noise.

showcasing its interpretability, flexibility, and broad applicability.

(3) Deep Learning for Imaging Depth Enhancement in PAM Reconstruction

In clinical settings, imaging deep tissues is essential, and neural networks play a key role in enhancing imaging depth.

Traditional AR-PAM systems face challenges with poor reconstruction in deep or out-of-focus regions. Meng *et al.* developed ResUnet-AG [94] a Residual U-Net with an attention mechanism, which enhances deeper tissue imaging by ignoring background noise, extending the depth of field from 1 to 3 mm.

A pyramid structure fusion concept has been proposed to significantly boost imaging depth. To enhance PAI speed, computational methods are being explored, as the laser pulse

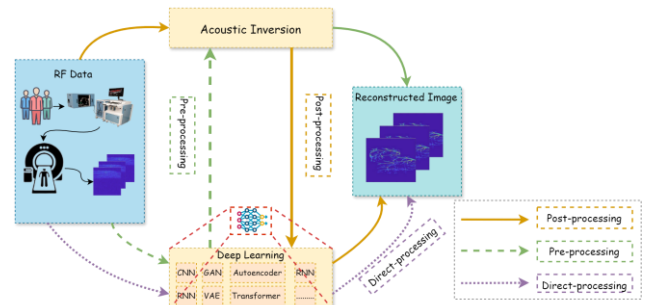


Fig. 6. Paradigm illustration using deep learning for PACT reconstruction.

repetition rate limits PAM speed. Loc *et al.* introduced DiffPam [95], a diffusion model-based algorithm that accelerates PAI, matching U-Net models' performance without large datasets or training. Additionally, shortening the diffusion process reduces computational time without affecting accuracy. Table 7 summarizes PAM reconstruction approaches.

3) PAE Image Reconstruction

Endoscopy is essential for diagnosing internal organ diseases, but its images often struggle to differentiate microvessels or identify lesions due to internal environmental and imaging conditions [13]. faces challenges with limited fields of view and complex in vivo environments. Factors such as blood, illumination variations, specular reflections, and smoke introduce noise, degrading image quality, especially in occluded regions. Enhancing endoscopic image quality by improving details, contrast, brightness, and removing specular reflections is crucial [96].

Yeung introduced Focus U-Net [97], a dual attention-gated deep neural network that selectively learns polyp features, incorporating skip connections, deep supervision, and a Hybrid Focal Loss to address class imbalance. This network holds promise for noninvasive colorectal cancer screening and other biomedical image segmentation tasks.

In clinical surgery, noise degrades endoscopic images. Zhang *et al.* [98] introduced an improved weighted guided filtering model to enhance vessel details and contours by boosting detail, contrast, and brightness, while removing highlight areas. This method suppresses noise, preserves the original image structure, and enhances the visibility of tissue vessels, providing insights for endoscopy device development.

Building on this, Moghtaderi *et al.* [99] developed a technique that generates three complementary sub-images using Contrast Limited Adaptive Histogram Equalization (CLAHE), image brightening, and detail enhancement. These sub-images are decomposed via multi-level wavelet transforms and guided filters, then fused with weights to produce a final enhanced image, suitable for low-light conditions in endoscopy.

Improving the resolution and SNR in defocused regions is crucial for designing advanced ultrasound/photoacoustic endoscopy systems. Wang *et al.* [100] introduced a novel reconstruction algorithm based on an approximate Gaussian acoustic field, which enhances the resolution and SNR in out-of-focus areas. This algorithm was validated using a chicken breast phantom and in a rabbit rectal endoscopy experiment, demonstrating improved imaging quality, faster dynamic focusing, and enhanced overall imaging performance.

Molecular photoacoustic endoscopic (PAE) imaging in deep tissues faces significant technical challenges. Xiao *et al.* [101] developed an improved back-projection (IBP) algorithm for focused detection over centimeter-scale imaging depths and employed a deep-learning-based method to reduce electrical noise from the step motor. These advancements decrease scanning time and foster the development of high-penetration molecular PAE.

V. DEEP LEARNING-BASED QUANTITATIVE ANALYSIS IN PHOTOACOUSTIC IMAGING

PAI offers comprehensive structural, functional, molecular, and kinetic information using both endogenous agents, such as hemoglobin, lipids, melanin, and water, and various exogenous agents. A key feature of PAI is its ability to differentiate between deoxy-hemoglobin (Hb) and oxy-hemoglobin (HbO₂), enabling the measurement of oxygen saturation (sO₂) in blood vessels, which is crucial for detecting physiological states like ischemia, hypoxia, or hypoxemia [102]. Additionally, PAI

leverages the optical absorption properties of melanin to image melanoma, pigmented lesions, and hair follicles. Clinically relevant, FDA-approved contrast agents, including ICG and methylene blue, which exhibit strong photoacoustic properties, are valuable in PAI applications [20]. Therefore, quantitative analysis in PAI is essential and involves optical fluence compensation and spectral unmixing [103].

A. Optical Fluence Compensation

The accuracy and clinical effectiveness of quantitative PAI (qPAI) are influenced by the spatial distribution of optical fluence, which varies with depth and wavelength. Optical fluence compensation corrects image distortions caused by inhomogeneous light distribution, enhancing the accuracy of physiological parameters such as hemoglobin concentration and oxygen saturation. DL models can learn complex feature representations from raw data and train networks to estimate and compensate for fluence differences due to variations in tissue optical properties. This approach can automatically and efficiently handle the compensation task, thereby improving the quality of image reconstruction. To address this, compensation methods include model-based methods, iterative compensation methods, multimodal approaches, deep learning-based methods, and other fluence compensation techniques [103].

1) Model-based Methods

Several models of light transport are used to determine optical fluence, including the photon diffusion equation (PDE), Monte Carlo (MC) models based on the radiative transfer equation (RTE) [104], and the diffusion dipole model (DDM) [105]. PDE is suitable for macroscopic descriptions, as demonstrated by Zhao *et al.* with FEA-generated fluence maps [106]. MC simulations, employed by Kirillin *et al.* [107] and Hirasawa *et al.* [108], model individual photons and mitigate spectral coloring. Ranasinghesagara *et al.* [109] used multi-illumination PA microscopy (MI-PAM) to measure optical properties, which were then input into an MC model to calculate fluence.

2) Iterative Compensation Methods

Iterative fluence compensation refines fluence distribution through an optimization process, starting with an initial estimate and updating it iteratively to match observed photoacoustic signals until convergence. This method does not require prior knowledge of optical parameters, making it more robust and accurate than model-based methods, which can introduce biases with inaccurate parameters. Iterative algorithms adapt well to complex conditions but demand high computational resources, especially with 3D data or MC models [110]. While minimizing iterations is ideal, achieving higher accuracy often necessitates more iterations or a more sophisticated algorithm, presenting a trade-off between accuracy and computational demands.

3) Multimodal Approaches

USI in combination with PAI can provide dual-modality imaging, using structural information to improve fluence maps and photoacoustic image quality [111]. However, USI requires time-consuming segmentation and identification, which may need experienced clinicians. AI-based segmentation can reduce the time cost, but processing ultrasound images, especially in 3D, demands significant computational resources. Diffuse optical tomography (DOT) also reconstructs 3D maps of tissue

optical properties to enhance fluence accuracy in deep tissue PAI. While DOT shares benefits with USI, it similarly requires additional optical equipment and extensive processing, increasing computational demands.

4) Deep Learning-based Methods

A relatively new method for optical fluence compensation in photoacoustic images is deep learning. For instance, Yang *et al.* [102] used a deep residual recurrent neural network (DR2U-Net) to estimate sO₂ levels in photoacoustic images. However, the accuracy and generalizability of DL models depend on having sufficient photoacoustic data. Training these models requires substantial computational resources and time, and complex architectures can lead to longer processing times.

5) Other Fluence Compensation Methods

Another method used to compensate for optical fluence variations is wavefront shaping. In a study by Caravaca-Aguirre *et al.*, a spatial light modulator (SLM) was used to modulate the wavefront of a 532 nm laser beam before it was focused onto two capillary tubes behind a glass diffuser [112]. To improve the measurement of sO₂ using photoacoustic images, Fadhel *et al.* developed a fluence matching algorithm to correct errors in raw photoacoustic images arising from wavelength-dependent fluence variations [113].

B. Spectral Unmixing

Spectral unmixing is a technique that decomposes signals from multiple absorbers within a pixel, facilitating the quantification of individual chromophores such as oxy- and deoxyhemoglobin, lipid content, and melanin. Photoacoustic (PA) data is typically acquired across several wavelengths, resulting in multispectral images that encapsulate mixed information from various chromophores [114], [115]. Applying deep learning for spectral unmixing can enhance the separation of different absorbers from these mixed signals. By training deep learning models to identify and isolate the spectral signatures of diverse absorptive substances, more accurate quantitative analyses can be achieved. Despite the complexity of tissue composition, spectral unmixing techniques have proven effective in distinguishing these chromophores. As its name suggests, the spectral unmixing technique aims to decode mixed pixels into a set of end members by determining the contribution of each end member to the observed spectrum at each pixel location [116].

1) Linear Spectral Fitting

Traditional approaches to solving the spectral unmixing problem typically involve a linear regression algorithm which assumes that each pixel in the photoacoustic image represents a linear combination of absorption and concentration of different chromophores, i.e., the linear mixing model (LMM) [117]. Feng *et al.* demonstrated collagen as a biomarker for bone health assessment using multi-wavelength PA (MWPA) [118]. While conventional linear spectral fitting partially addresses this problem, it is limited by the availability of known absorption spectra and the spectral coloring effects observed in complex tissues [115].

2) Statistical Detection Method

Statistical detection methods focus on identifying specific target spectra without requiring explicit knowledge of background absorption spectra. This makes them ideal for detecting molecules with known spectra, such as exogenous

nanoparticles, reporter genes, and oxy- and deoxy-hemoglobin. For example, Tzoumas *et al.* [119] introduced eigenspectra multispectral optoacoustic tomography (eMSOT) to estimate oxygen saturation (sO₂) levels in vivo. These methods typically rely on large datasets, which can increase computational demands and pose challenges, especially in the case of in vivo measurements.

3) Blind Source Unmixing

The exploration of various blind source unmixing algorithms holds promise in mitigating the challenges of linear spectral unmixing and enhancing the precision of qPAI. More importantly, blind source unmixing is a method capable of separating images without relying on prior knowledge of spectral signatures or fluence distribution. This technique possesses the capability to recover unknown source "signals" solely based on the understanding of observed mixtures of these signals within an image, which is particularly suitable to study complex biological tissues [120].

4) Learning-based Spectral Unmixing

Kirchner *et al.* developed context-enhanced quantitative photoacoustic imaging (CE-qPAI) using Monte Carlo simulations and random forests to enhance spectral unmixing [121]. Cai *et al.* introduced an end-to-end ResU-net approach for accurate quantitative imaging in simulations. Gröhl's team used LSD with a neural network to improve oxygenation estimation accuracy [122]. Olefir *et al.* [123] enhanced MSOT with DL-eMSOT, achieving superior performance using synthetic data.

In addressing the challenges of qPAI, it is essential to account for spatial variations in optical fluence to derive accurate absorption maps (shown in Fig. 7). Strategies include model-based methods, iterative compensation, multimodal approaches, and deep-learning techniques. Robust spectral unmixing is also critical for accurately obtaining physiological and biochemical information at depth. Recent advancements such as linear spectral fitting, statistical detection methods, blind source unmixing, and learning-based approaches have significantly improved the decoding of mixed pixel information into distinct chromophores. Notably, the challenges in qPAI are often interconnected due to the hybrid nature of optical absorption and acoustic detection; recognizing this interdependence is beneficial for developing effective strategies to enhance qPAI's reliability and applicability across various biomedical contexts.

VI. FUTURE WORK

The clinical applications of photoacoustic imaging (PAI) have been extensively studied, with the International Photoacoustic Standardization Consortium advocating for standardization in data management, hardware testing, and clinical utilization. Despite receiving approvals from the FDA and CE, as well as being incorporated into the DICOM standard [7], PAI still faces several challenges, including limited optical penetration depth, high equipment costs, and concerns regarding patient safety [124]. Ongoing advancements in hardware and software technologies, coupled with the integration of artificial intelligence (AI) to enhance imaging quality, depth resolution, and acquisition speed, are anticipated to mitigate these issues. Consequently, future research should concentrate on the following critical areas.

A. Single Image Super-Resolution in PAI

High-resolution photoacoustic (PA) images are essential for clinical applications and image analysis, but hardware limitations often necessitate trade-offs in scan time, SNR, and spatial coverage. DL-based super-resolution techniques, extensively researched in other modalities, enhance PA image reconstruction by iterative optimization gradient flow, improving model stability, and capturing detailed information. These techniques integrate dense connections and feedback mechanisms to leverage prior information for self-correction, leading to stable iterative optimization and accelerated model convergence, thus improving reconstruction fidelity.

Implementing super-resolution techniques in PAE imaging enhances diagnostic value and analytical precision without necessitating costly hardware upgrades. Advanced DL models tailored for super-resolution tasks enable higher-fidelity reconstructions, offering clearer visualizations of anatomical structures and potential pathologies. Since Dong *et al.*'s pioneering work in 2014 [125], optimized models such as SRCNN [126], SRGAN [127], CAMixerSR [128], and CoSeR [129] have emerged, showcasing significant progress within super-resolution technology domain specifically applicable across medical imaging contexts. Furthermore deep-structured networks like VDSR [130], DRRN [131], RFDN [132] combined with innovative frameworks exemplified by the Deep Multi-Scale Network (DMSN) [133] have further enhanced quality metrics associated with existing SR methods utilized throughout healthcare settings.

B. Physics-Informed Reconstruction in PAI

Using deep learning for PAI presents challenges such as managing incomplete datasets and the high computational costs associated with large training requirements. To address these issues, physics-informed DL approaches have been developed. These methods integrate physical models with AI to enhance reconstruction quality and reduce processing time. By incorporating physical constraints and prior knowledge, these approaches improve the performance and robustness of DL architectures. Notable examples include PAT-MDAE [75] and the physics-driven DL-based filtered back projection (dFBP) framework [134], which demonstrate significant potential for advancing biomedical PAI applications.

C. Deep Learning-Based Multimodal Fusion in PAI

Multimodal imaging systems, combining PAI with OCT, ultrasound, and other modalities, enhance imaging depth and spatial resolution, providing comprehensive tissue information [135]. Multimodal image-guided surgical navigation, integrating techniques such as endoscopy, ultrasound, and fluorescence, improves visualization and spatial identification of critical structures, supporting minimally invasive procedures in neurosurgery, orthopedics, and vascular interventions. Key technologies include multimodal image segmentation, surgical planning, position calibration, image registration, and multi-source information fusion. Recent advancements in image fusion techniques, such as GANMcC [136], leverage GANs alongside Transformers to effectively integrate gradient and intensity information. Nyayapathi *et al.* [137] proposed a novel architecture that integrates both Transformer and CNN elements, featuring global and local branches within the

encoder module. Furthermore, the combination of photoacoustic/ultrasound systems with methods like diffuse optical tomography and MRI enhances disease monitoring and diagnosis; this is particularly beneficial for brain imaging aimed at obtaining functional and molecular insights through MRI. Anatomical data derived from ultrasound improves the lateral resolution of PAI systems, enabling detailed visualization of cerebral vasculature [138]. Additionally, it is crucial to evaluate these fusion technologies in clinical settings to ensure their continued advancement [139].

D. Quantitative Analysis in PAI

Future research on qPAI will focus on enhancing luminous flux modeling for precise tissue absorption coefficient reconstruction, improving spectral unmixing with advanced methods, and developing unsupervised super-resolution models to address data scarcity. Efforts will also include creating compact and efficient network models, innovating evaluation metrics aligned with human perception, and deepening DL theory for better reliability and interpretability. Advances in reconstruction techniques will address limited view and acoustic heterogeneity while enabling real-time reconstruction using deep learning. Integrating qPAI with other modalities will improve resolution and contrast. Clinical trials will establish efficacy and safety, while new contrast agents, portable systems, and functional/molecular imaging extensions will further advance qPAI in biomedical research and clinical diagnosis [140].

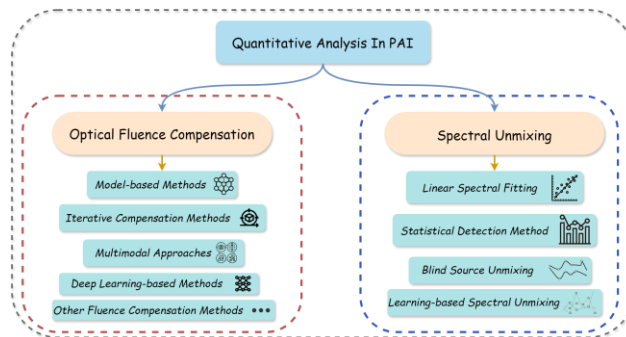


Fig. 7. Overview of quantitative analysis of PAI.

VII. CONCLUSION

PAI has emerged as a powerful technique for achieving high-resolution visualization of optical contrast within biological tissues, effectively addressing the limitations of traditional optical imaging methods. Over the past decade, extensive research has demonstrated PAI's advantages in disease screening, diagnosis, and monitoring across various organs. This review begins by elucidating the foundational principles of PAI and its superiority over OCT and US. It then explores the constraints of conventional approaches and highlights the pivotal role of deep learning in advancing PACT, PAM, and PAE. Implementing AI-driven techniques is essential for reducing image degradation caused by limited spatial sampling in PAI. These tailored methods, adaptable to diverse system configurations, sampling conditions, and imaging targets, significantly reduce artifacts, enhance anatomical visibility, improve wave source localization, and facilitate precise

quantitative assessments. Addressing spatial variations in optical fluence is critical for accurately deriving absorption maps during tissue imaging. Similarly, robust spectral unmixing is indispensable for obtaining precise physiological and biochemical data at depth. Overcoming these challenges is key to expanding the clinical applications of PAI. The review concludes by exploring future research directions, including single-image super-resolution, physics-informed deep learning, multimodal image fusion, and quantitative analysis, emphasizing the transformative impact of deep learning on the field's ongoing evolution.

VIII. COMPETING INTERESTS

The authors declare no competing interests.

REFERENCES

- [1] A. A. Oraevsky *et al.*, "Laser-based photoacoustic imaging in biological tissues," in *Laser-Tissue Interaction V; and Ultraviolet Radiation Hazards*, Los Angeles, United States: SPIE, Aug. 1994, p. 16.
- [2] T. P. Matthews and M. A. Anastasio, "Joint reconstruction of the initial pressure and speed of sound distributions from combined photoacoustic and ultrasound tomography measurements," *Inverse Problems*, vol. 33, no. 12, p. 124002, Dec. 2017.
- [3] L. V. Wang, "Tutorial on Photoacoustic Microscopy and Computed Tomography," *IEEE J. Select. Topics Quantum Electron.*, vol. 14, no. 1, pp. 171–179, 2008.
- [4] J. Poudel *et al.*, "A survey of computational frameworks for solving the acoustic inverse problem in three-dimensional photoacoustic computed tomography," *Phys. Med. Biol.*, vol. 64, no. 14, July. 2019.
- [5] B. Ning *et al.*, "Ultrasound-aided Multi-parametric Photoacoustic Microscopy of the Mouse Brain," *Sci Rep*, vol. 5, no. 1, p. 18775, Dec. 2015.
- [6] S. Zackrisson *et al.*, "Light In and Sound Out: Emerging Translational Strategies for Photoacoustic Imaging," *Cancer Research*, vol. 74, no. 4, pp. 979–1004, Feb. 2014.
- [7] J. Park *et al.*, "Clinical translation of photoacoustic imaging," *Nat Rev Bieng.*, Sep. 2024.
- [8] S. Park *et al.*, "Contrast-enhanced dual mode imaging: photoacoustic imaging plus more," *Biomed. Eng. Lett.*, vol. 7, no. 2, pp. 121–133, May 2017.
- [9] P. Rajendran *et al.*, "Photoacoustic imaging aided with deep learning: a review," *Biomed. Eng. Lett.*, vol. 12, no. 2, pp. 155–173, May 2022.
- [10] A. DiSpirito *et al.*, "Sounding out the hidden data: A concise review of deep learning in photoacoustic imaging," *Exp Biol Med (Maywood)*, vol. 246, no. 12, pp. 1355–1367, Jun. 2021.
- [11] J. Park *et al.*, "Quadruple ultrasound, photoacoustic, optical coherence, and fluorescence fusion imaging with a transparent ultrasound transducer," *Proc. Natl. Acad. Sci. U.S.A.*, vol. 118, no. 11, p. e1920879118, Mar. 2021.
- [12] R. R. Gharieb, Ed., 'Photoacoustic Imaging - Principles, Advances and Applications'. IntechOpen, May 06, 2020, 124.
- [13] H. Guo *et al.*, "Photoacoustic endoscopy: A progress review," *Journal of Biophotonics*, vol. 13, no. 12, p. e202000217, Dec. 2020.
- [14] B. Cox *et al.*, "Quantitative spectroscopic photoacoustic imaging: a review," *J. Biomed. Opt.*, vol. 17, no. 6, p. 061202, 2012.
- [15] J. Xia *et al.*, "PHOTOACOUSTIC TOMOGRAPHY: PRINCIPLES AND ADVANCES (Invited Review)," *PIER*, vol. 147, pp. 1–22, 2014.
- [16] S. Park *et al.*, "Real-time Triple-modal Photoacoustic, Ultrasound, and Magnetic Resonance Fusion Imaging of Humans," *IEEE Trans. Med. Imaging*, vol. 36, no. 9, pp. 1912–1921, Sep. 2017.
- [17] S. Mallidi *et al.*, "Photoacoustic imaging in cancer detection, diagnosis, and treatment guidance," *Trends in Biotechnology*, vol. 29, no. 5, pp. 213–221, May 2011.
- [18] P. Beard, "Biomedical photoacoustic imaging," *Interface Focus.*, vol. 1, no. 4, pp. 602–631, Aug. 2011.
- [19] Y. Yu *et al.*, "Simultaneous photoacoustic and ultrasound imaging: A review," *Ultrasonics*, vol. 139, p. 107277, Apr. 2024.
- [20] L. V. Wang, "Multiscale photoacoustic microscopy and computed tomography," *Nature Photon.*, vol. 3, no. 9, pp. 503–509, Sep. 2009.
- [21] C. Liu *et al.*, "The integrated high-resolution reflection-mode photoacoustic and fluorescence confocal microscopy," *Photoacoustics*, vol. 14, pp. 12–18, Jun. 2019.
- [22] A. B. E. Attia *et al.*, "A review of clinical photoacoustic imaging: Current and future trends," *Photoacoustics*, vol. 16, p. 100144, Dec. 2019.
- [23] M. Omar *et al.*, "Photoacoustic mesoscopy for biomedicine," *Nat Biomed Eng.*, vol. 3, no. 5, pp. 354–370, Apr. 2019.
- [24] M. Moothanchery and M. Pramanik, "Performance Characterization of a Switchable Acoustic Resolution and Optical Resolution Photoacoustic Microscopy System," *Sensors*, vol. 17, no. 2, p. 357, Feb. 2017.
- [25] L. Lin and L. V. Wang, "The emerging role of photoacoustic imaging in clinical oncology," *Nat Rev Clin Oncol.*, vol. 19, no. 6, pp. 365–384, Jun. 2022.
- [26] L. Li and L. V. Wang, "Recent Advances in Photoacoustic Tomography," *BME Front.*, vol. 2021, p. 9823268, Jan. 2021.
- [27] S. Na and L. V. Wang, "Photoacoustic computed tomography for functional human brain imaging [Invited]," *Biomed. Opt. Express*, vol. 12, no. 7, p. 4056, Jul. 2021.
- [28] A. Q. Bauer *et al.*, "Quantitative photoacoustic imaging: correcting for heterogeneous light fluence distributions using diffuse optical tomography," *J. Biomed. Opt.*, vol. 16, no. 9, p. 096016, 2011.
- [29] C. Tian *et al.*, "Spatial resolution in photoacoustic computed tomography," *Rep. Prog. Phys.*, vol. 84, no. 3, p. 036701, Mar. 2021.
- [30] M. Jeon and C. Kim, "Multimodal Photoacoustic Tomography," *IEEE Trans. Multimedia*, vol. 15, no. 5, pp. 975–982, Aug. 2013.
- [31] S. Jeon *et al.*, "Review on practical photoacoustic microscopy," *Photoacoustics*, vol. 15, p. 100141, Sep. 2019.
- [32] T. Vu *et al.*, "A generative adversarial network for artifact removal in photoacoustic computed tomography with a linear-array transducer," *Exp Biol Med (Maywood)*, vol. 245, no. 7, pp. 597–605, Apr. 2020.
- [33] I. Steinberg *et al.*, "Photoacoustic clinical imaging," *Photoacoustics*, vol. 14, pp. 77–98, Jun. 2019.
- [34] P. Rajendran and M. Pramanik, "Deep learning approach to improve tangential resolution in photoacoustic tomography," *Biomed. Opt. Express*, vol. 11, no. 12, p. 7311, Dec. 2020.
- [35] S. Zhang *et al.*, "Challenges and advances in two-dimensional photoacoustic computed tomography: a review," *J. Biomed. Opt.*, vol. 29, no. 07, Jul. 2024.
- [36] C. Tian, M. Pei *et al.*, "Impact of System Factors on the Performance of Photoacoustic Tomography Scanners," *Phys. Rev. Applied*, vol. 13, no. 1, p. 014001, Jan. 2020.
- [37] J. Yao and L. V. Wang, "Perspective on fast-evolving photoacoustic tomography," *J. Biomed. Opt.*, vol. 26, no. 06, Jun. 2021.
- [38] Y. Zhou *et al.*, "Tutorial on photoacoustic tomography," *J. Biomed. Opt.*, vol. 21, no. 6, p. 061007, Apr. 2016.
- [39] Z. Balci and A. Mert, "Enhanced photoacoustic signal processing using empirical mode decomposition and machine learning," *Nondestructive Testing and Evaluation*, pp. 1–13, Jun. 2024.
- [40] J. Yao and L. V. Wang, "Photoacoustic microscopy," *Laser & Photonics Reviews*, vol. 7, no. 5, pp. 758–778, Sep. 2013.
- [41] K. M. Kempinski *et al.*, "Application of the generalized contrast-to-noise ratio to assess photoacoustic image quality," *Biomed. Opt. Express*, vol. 11, no. 7, p. 3684, Jul. 2020.
- [42] Q. Chen *et al.*, "Progress of clinical translation of handheld and semi-handheld photoacoustic imaging," *Photoacoustics*, vol. 22, p. 100264, Jun. 2021.
- [43] K.-T. Hsu *et al.*, "Comparing Deep Learning Frameworks for Photoacoustic Tomography Image Reconstruction," *Photoacoustics*, vol. 23, p. 100271, Sep. 2021.
- [44] T.-J. Yoon, "Recent advances in photoacoustic endoscopy," *WJGE*, vol. 5, no. 11, p. 534, 2013.
- [45] M. Seong and S.-L. Chen, "Recent advances toward clinical applications of photoacoustic microscopy: a review," *Sci. China Life Sci.*, vol. 63, no. 12, pp. 1798–1812, Dec. 2020.
- [46] A. A. Oraevsky, "Image reconstruction from photoacoustic projections," *Photonics Insights*, vol. 3, no. 4, p. C06, 2024.
- [47] Y. Xu and L. V. Wang, "Time Reversal and Its Application to Tomography with Diffracting Sources," *Phys. Rev. Lett.*, vol. 92, no. 3, p. 033902, Jan. 2004.
- [48] P. Burgholzer *et al.*, "Exact and approximative imaging methods for photoacoustic tomography using an arbitrary detection surface," *Phys. Rev. E*, vol. 75, no. 4, p. 046706, Apr. 2007.
- [49] C. G. A. Hoelen *et al.*, "Three-dimensional photoacoustic imaging of blood vessels in tissue," *Opt. Lett.*, vol. 23, no. 8, p. 648, Apr. 1998.

- [50] C. G. Hoelen *et al.*, “Photoacoustic blood cell detection and imaging of blood vessels in phantom tissue,” presented at the BIOS Europe '97, H.-J. Foth, R. Marchesini, H. Podbielska, and A. Katzir, Eds., San Remo, Italy, Jan. 1998, pp. 142–153.
- [51] R. A. Kruger *et al.*, “Photoacoustic ultrasound (PAUS)—Reconstruction tomography,” *Medical Physics*, vol. 22, no. 10, pp. 1605–1609, Oct. 1995.
- [52] Y. Guo *et al.*, “Deep learning for visual understanding: A review,” *Neurocomputing*, vol. 187, pp. 27–48, Apr. 2016.
- [53] M. Xu and L. V. Wang, “Universal back-projection algorithm for photoacoustic computed tomography,” *Phys. Rev. E*, vol. 71, no. 1, p. 016706, Jan. 2005.
- [54] C.-H. Tai *et al.*, “SE: an algorithm for deriving sequence alignment from a pair of superimposed structures,” *BMC Bioinformatics*, vol. 10, no. S1, p. S4, Jan. 2009.
- [55] R. Wang *et al.*, “Photoacoustic imaging with limited sampling: a review of machine learning approaches,” *Biomed. Opt. Express*, vol. 14, no. 4, p. 1777, Apr. 2023.
- [56] H. Shan *et al.*, “Simultaneous reconstruction of the initial pressure and sound speed in photoacoustic tomography using a deep-learning approach,” in *Novel Optical Systems, Methods, and Applications XXII*, C. F. Hahlweg and J. R. Mulley, Eds., San Diego, United States: SPIE, Sep. 2019, p. 4.
- [57] S. Ravishankar *et al.*, “Image Reconstruction: From Sparsity to Data-Adaptive Methods and Machine Learning,” *Proc. IEEE*, vol. 108, no. 1, pp. 86–109, Jan. 2020.
- [58] N. Davoudi *et al.*, “Deep learning optoacoustic tomography with sparse data,” *Nat Mach Intell*, vol. 1, no. 10, pp. 453–460, Sep. 2019.
- [59] Antholzer, S *et al.*, “Photoacoustic image reconstruction via deep learning,” in *Photons Plus Ultrasound: Imaging and Sensing 2018*, eds. A. A. Oraevsky and L. V. Wang, San Francisco, United States: SPIE, Feb. 2018, pp. 168.
- [60] X. Wei *et al.*, “Deep learning-powered biomedical photoacoustic imaging,” *Neurocomputing*, vol. 573, p. 127207, Mar. 2024.
- [61] C. Yang *et al.*, “Review of deep learning for photoacoustic imaging,” *Photoacoustics*, vol. 21, p. 100215, Mar. 2021.
- [62] Q. Huang *et al.*, “A review of deep learning segmentation methods for carotid artery ultrasound images,” *Neurocomputing*, vol. 545, p. 126298, Aug. 2023.
- [63] J. Schmidhuber, “Deep learning in neural networks: An overview,” *Neural Networks*, vol. 61, pp. 85–117, Jan. 2015.
- [64] O. Ronneberger *et al.*, “U-Net: Convolutional Networks for Biomedical Image Segmentation,” in *Medical Image Computing and Computer-Assisted Intervention – MICCAI 2015*, vol. 9351, N. Navab, J. Hornegger, W. M. Wells, and A. F. Frangi, Eds., in Lecture Notes in Computer Science, vol. 9351, Cham: Springer International Publishing, 2015, pp. 234–241.
- [65] D. Allman *et al.*, “Photoacoustic Source Detection and Reflection Artifact Removal Enabled by Deep Learning,” *IEEE Trans. Med. Imaging*, vol. 37, no. 6, pp. 1464–1477, Jun. 2018.
- [66] S. Gutta *et al.*, “Deep neural network-based bandwidth enhancement of photoacoustic data,” *J. Biomed. Opt.*, vol. 22, no. 11, p. 1.
- [67] N. Awasthi *et al.*, “Deep Neural Network-Based Sinogram Super-Resolution and Bandwidth Enhancement for Limited-Data Photoacoustic Tomography,” *IEEE Trans. Ultrason., Ferroelect., Freq. Contr.*, vol. 67, no. 12, pp. 2660–2673, Dec. 2020.
- [68] D. A. Durairaj *et al.*, “Unsupervised deep learning approach for photoacoustic spectral unmixing,” in *Photons Plus Ultrasound: Imaging and Sensing 2020*, A. A. Oraevsky and L. V. Wang, Eds., San Francisco, United States: SPIE, Feb. 2020, p. 125.
- [69] J. Feng *et al.*, “End-to-end Res-Unet based reconstruction algorithm for photoacoustic imaging,” *Biomed. Opt. Express*, vol. 11, no. 9, p. 5321, Sep. 2020.
- [70] S. Guan *et al.*, “Fully Dense UNet for 2-D Sparse Photoacoustic Tomography Artifact Removal,” *IEEE J. Biomed. Health Inform.*, vol. 24, no. 2, pp. 568–576, Feb. 2020.
- [71] J. Zhang *et al.*, “Limited-View Photoacoustic Imaging Reconstruction With Dual Domain Inputs Based On Mutual Information,” in *2021 IEEE 18th International Symposium on Biomedical Imaging (ISBI)*, Nice, France: IEEE, Apr. 2021, pp. 1522–1526.
- [72] Lan H *et al.*, “A jointed feature fusion framework for photoacoustic image reconstruction,” *Photoacoustics*, Feb; 29:100442, 2023.
- [73] D. Zhang and A. Khoreva, “Progressive Augmentation of GANs,” *arXiv: 1901.10422*, 2019.
- [74] W. Zhong *et al.*, “Unsupervised disentanglement strategy for mitigating artifact in photoacoustic tomography under extremely sparse view,” *Photoacoustics*, vol. 38, p. 100613, Aug. 2024.
- [75] X. Song *et al.*, “Accelerated model-based iterative reconstruction strategy for sparse-view photoacoustic tomography aided by multi-channel autoencoder priors,” *Journal of Biophotonics*, vol. 17, no. 1, p. e202300281, Jan. 2024.
- [76] M. Guo *et al.*, “AS-Net: Fast Photoacoustic Reconstruction With Multi-Feature Fusion From Sparse Data,” *IEEE Trans. Comput. Imaging*, vol. 8, pp. 215–223, 2022.
- [77] S. C. K. Chan *et al.*, “Local Spatial Attention Transformer For Sparse Photoacoustic Image Reconstruction,” in *2024 IEEE International Symposium on Biomedical Imaging (ISBI)*, Athens, Greece: IEEE, May 2024, pp. 1–5.
- [78] T. Tong *et al.*, “Domain Transform Network for Photoacoustic Tomography from Limited-view and Sparsely Sampled Data,” *Photoacoustics*, vol. 19, p. 100190, Sep. 2020.
- [79] H. Lan *et al.*, “Y-Net: Hybrid deep learning image reconstruction for photoacoustic tomography in vivo,” *Photoacoustics*, vol. 20, p. 100197, Dec. 2020.
- [80] T. Vu *et al.*, “Deep image prior for undersampling high-speed photoacoustic microscopy,” 2020.
- [81] D. Seong *et al.*, “Three-dimensional reconstructing undersampled photoacoustic microscopy images using deep learning,” *Photoacoustics*, vol. 29, p. 100429, Feb. 2023.
- [82] B. Li *et al.*, “Removing Artifacts in Transcranial Photoacoustic Imaging With Polarized Self-Attention Dense-UNet,” *Ultrasound in Medicine & Biology*, vol. 50, no. 10, pp. 1530–1543, Oct. 2024.
- [83] J. Wang *et al.*, “Reconstructing Cancellous Bone From Down-Sampled Optical-Resolution Photoacoustic Microscopy Images With Deep Learning,” *Ultrasound in Medicine & Biology*, vol. 50, no. 9, pp. 1459–1471, Sep. 2024.
- [84] H. Shahid *et al.*, “Batch ReNormalization Accumulated Residual U-Net for Artifacts Removal in Photoacoustic Imaging,” in *2021 IEEE International Ultrasonics Symposium (IUS)*, Xi’an, China: IEEE, Sep. 2021, pp. 1–4.
- [85] Y. Cao *et al.*, “Mean-reverting diffusion model-enhanced acoustic-resolution photoacoustic microscopy for resolution enhancement: Toward optical resolution,” *J. Innov. Opt. Health Sci.*, p. 2450023, Sep. 2024.
- [86] T. D. Le *et al.*, “Enhanced resolution and sensitivity acoustic-resolution photoacoustic microscopy with semi/unsupervised GANs,” *Sci Rep*, vol. 13, no. 1, p. 13423, Aug. 2023.
- [87] S. Cheng *et al.*, “High-resolution photoacoustic microscopy with deep penetration through learning,” *Photoacoustics*, vol. 25, p. 100314, Mar. 2022.
- [88] H. Zhao *et al.*, “Deep Learning Enables Superior Photoacoustic Imaging at Ultralow Laser Dosages,” *Advanced Science*, vol. 8, no. 3, p. 2003097, Feb. 2021.
- [89] M. Zhou *et al.*, “A Noise Reduction Method for Photoacoustic Imaging In Vivo Based on EMD and Conditional Mutual Information,” *IEEE Photonics J.*, vol. 11, no. 1, pp. 1–10, Feb. 2019.
- [90] Y. Liu *et al.*, “UPAMNet: A unified network with deep knowledge priors for photoacoustic microscopy,” *Photoacoustics*, vol. 38, p. 100608, Aug. 2024.
- [91] D. He *et al.*, “De-Noising of Photoacoustic Microscopy Images by Attentive Generative Adversarial Network,” *IEEE Trans. Med. Imaging*, vol. 42, no. 5, pp. 1349–1362, May 2023.
- [92] J. Zhang *et al.*, “Organ-PAM: Photoacoustic Microscopy of Whole-organ Multiset Vessel Systems,” *Laser & Photonics Reviews*, vol. 17, no. 7, p. 2201031, Jul. 2023.
- [93] Z. Zhang *et al.*, “Adaptive enhancement of acoustic resolution photoacoustic microscopy imaging via deep CNN prior,” *Photoacoustics*, vol. 30, p. 100484, Apr. 2023.
- [94] J. Meng *et al.*, “Depth-extended acoustic-resolution photoacoustic microscopy based on a two-stage deep learning network,” *Biomed. Opt. Express*, vol. 13, no. 8, p. 4386, Aug. 2022.
- [95] I. Loc and M. B. Unlu, “Speeding up Photoacoustic Imaging using Diffusion Models,” *arXiv: 2312.08834*, Oct. 17, 2024.
- [96] W. Li *et al.*, “EndoSRR: a comprehensive multi-stage approach for endoscopic specular reflection removal,” *Int J CARS*, vol. 19, no. 6, pp. 1203–1211, Apr. 2024.
- [97] M. Yeung *et al.*, “Focus U-Net: A novel dual attention-gated CNN for polyp segmentation during colonoscopy,” *Computers in Biology and Medicine*, vol. 137, p. 104815, Oct. 2021.

- [98] G. Zhang *et al.*, “A Medical Endoscope Image Enhancement Method Based on Improved Weighted Guided Filtering,” *Mathematics*, vol. 10, no. 9, p. 1423, Apr. 2022.
- [99] S. Moghtaderi *et al.*, “Endoscopic Image Enhancement: Wavelet Transform and Guided Filter Decomposition-Based Fusion Approach,” *J. Imaging*, vol. 10, no. 1, p. 28, Jan. 2024.
- [100] Y. Wang *et al.*, “Photoacoustic/Ultrasound Endoscopic Imaging Reconstruction Algorithm Based on the Approximate Gaussian Acoustic Field,” *Biosensors*, vol. 12, no. 7, p. 463, Jun. 2022.
- [101] J. Xiao *et al.*, “Acoustic-resolution-based spectroscopic photoacoustic endoscopy towards molecular imaging in deep tissues,” *Opt. Express*, vol. 30, no. 19, p. 35014, Sep. 2022.
- [102] C. Yang *et al.*, “Quantitative Photoacoustic Blood Oxygenation Imaging Using Deep Residual And Recurrent Neural Network,” in *2019 IEEE 16th International Symposium on Biomedical Imaging (ISBI 2019)*, Venice, Italy: IEEE, Apr. 2019, pp. 741–744.
- [103] R. Zhang *et al.*, “Navigating challenges and solutions in quantitative photoacoustic imaging,” *Applied Physics Reviews*, vol. 11, no. 3, p. 031308, Sep. 2024.
- [104] M. Dantuma *et al.*, “Tunable blood oxygenation in the vascular anatomy of a semi-anthropomorphic photoacoustic breast phantom,” *J. Biomed. Opt.*, vol. 26, no. 03, Mar. 2021.
- [105] X. Zhou *et al.*, “Evaluation of Fluence Correction Algorithms in Multispectral Photoacoustic Imaging,” *Photoacoustics*, vol. 19, p. 100181, Sep. 2020.
- [106] L. Zhao *et al.*, “Optical fluence compensation for handheld photoacoustic probe: An *in vivo* human study case,” *J. Innov. Opt. Health Sci.*, vol. 10, no. 04, p. 1740002, Jul. 2017.
- [107] M. Kirillin *et al.*, “Fluence compensation in raster-scan photoacoustic angiography,” *Photoacoustics*, vol. 8, pp. 59–67, Dec. 2017.
- [108] T. Hirasawa *et al.*, “Multispectral photoacoustic imaging of tumours in mice injected with an enzyme-activatable photoacoustic probe,” *J. Opt.*, vol. 19, no. 1, p. 014002, Jan. 2017.
- [109] J. C. Ranasinghesagara *et al.*, “Reflection-mode multiple-illumination photoacoustic sensing to estimate optical properties,” *Photoacoustics*, vol. 2, no. 1, pp. 33–38, Mar. 2014.
- [110] H. Jin, R. Zhang *et al.*, “A Single Sensor Dual-Modality Photoacoustic Fusion Imaging for Compensation of Light Fluence Variation,” *IEEE Trans. Biomed. Eng.*, vol. 66, no. 6, pp. 1810–1813, Jun. 2019.
- [111] T. Han, M. Yang *et al.*, “A three-dimensional modeling method for quantitative photoacoustic breast imaging with handheld probe,” *Photoacoustics*, vol. 21, p. 100222, Mar. 2021.
- [112] A. M. Caravaca-Aguirre *et al.*, “High contrast three-dimensional photoacoustic imaging through scattering media by localized optical fluence enhancement,” *Opt. Express*, vol. 21, no. 22, p. 26671, Nov. 2013.
- [113] M. N. Fadhel *et al.*, “Fluence-matching technique using photoacoustic radiofrequency spectra for improving estimates of oxygen saturation,” *Photoacoustics*, vol. 19, p. 100182, Sep. 2020.
- [114] A. Dolet *et al.*, “In Vitro and In Vivo Multispectral Photoacoustic Imaging for the Evaluation of Chromophore Concentration,” *Sensors*, vol. 21, no. 10, p. 3366, May 2021.
- [115] M. U. Arabul *et al.*, “Unmixing multi-spectral photoacoustic sources in human carotid plaques using non-negative independent component analysis,” *Photoacoustics*, vol. 15, p. 100140, Sep. 2019.
- [116] C. Shi and L. Wang, “Incorporating spatial information in spectral unmixing: A review,” *Remote Sensing of Environment*, vol. 149, pp. 70–87, Jun. 2014.
- [117] S. Tzoumas and V. Ntziachristos, “Spectral unmixing techniques for photoacoustic imaging of tissue pathophysiology,” *Phil. Trans. R. Soc. A.*, vol. 375, no. 2107, p. 20170262, Nov. 2017.
- [118] T. Feng *et al.*, “Detection of collagen by multi-wavelength photoacoustic analysis as a biomarker for bone health assessment,” *Photoacoustics*, vol. 24, p. 100296, Dec. 2021.
- [119] S. Tzoumas *et al.*, “Eigenspectra photoacoustic tomography achieves quantitative blood oxygenation imaging deep in tissues,” *Nat Commun*, vol. 7, no. 1, p. 12121, Jun. 2016.
- [120] M. S. Karoui *et al.*, “Blind spatial unmixing of multispectral images: New methods combining sparse component analysis, clustering and non-negativity constraints,” *Pattern Recognition*, vol. 45, no. 12, pp. 4263–4278, Dec. 2012.
- [121] T. Kirchner *et al.*, “Context encoding enables machine learning-based quantitative photoacoustics,” *J. Biomed. Opt.*, vol. 23, no. 05, p. 1, May 2018.
- [122] C. Cai *et al.*, “End-to-end deep neural network for optical inversion in quantitative photoacoustic imaging,” *Opt. Lett.*, vol. 43, no. 12, p. 2752, Jun. 2018.
- [123] I. Olefir *et al.*, “Deep Learning-Based Spectral Unmixing for Photoacoustic Imaging of Tissue Oxygen Saturation,” *IEEE Trans. Med. Imaging*, vol. 39, no. 11, pp. 3643–3654, Nov. 2020.
- [124] N. T. Huynh *et al.*, “A fast all-optical 3D photoacoustic scanner for clinical vascular imaging,” *Nat. Biomed. Eng.*, Sep. 2024.
- [125] Dong, Chao *et al.* “Image Super-Resolution Using Deep Convolutional Networks.” *IEEE Transactions on Pattern Analysis and Machine Intelligence* 38 (2014): 295-307.
- [126] C. Dong *et al.*, “Learning a Deep Convolutional Network for Image Super-Resolution,” in *Computer Vision – ECCV 2014*, vol. 8692, D. Fleet, T. Pajdla, B. Schiele, and T. Tuytelaars, Eds., in Lecture Notes in Computer Science, vol. 8692, Cham: Springer International Publishing, 2014, pp. 184–199.
- [127] C. Ledig *et al.*, “Photo-Realistic Single Image Super-Resolution Using a Generative Adversarial Network,” in *2017 IEEE Conference on Computer Vision and Pattern Recognition (CVPR)*, Honolulu, HI: IEEE, Jul. 2017, pp. 105–114.
- [128] Y. Wang *et al.*, “CAMixerSR: Only Details Need More “Attention,”” 2024 IEEE/CVF Conference on Computer Vision and Pattern Recognition (CVPR), Seattle, WA, USA, 2024, pp. 25837-25846.
- [129] H. Sun *et al.*, “CoSeR: Bridging Image and Language for Cognitive Super-Resolution,” 2024 IEEE/CVF Conference on Computer Vision and Pattern Recognition (CVPR), Seattle, WA, USA, 2024, pp. 25868-25878.
- [130] J. Kim *et al.*, “Accurate Image Super-Resolution Using Very Deep Convolutional Networks,” in *2016 IEEE Conference on Computer Vision and Pattern Recognition (CVPR)*, Las Vegas, NV, USA: IEEE, Jun. 2016, pp. 1646–1654.
- [131] Y. Tai *et al.*, “Image Super-Resolution via Deep Recursive Residual Network,” in *2017 IEEE Conference on Computer Vision and Pattern Recognition (CVPR)*, Honolulu, HI: IEEE, Jul. 2017, pp. 2790–2798.
- [132] Liu *et al.*, “Residual Feature Distillation Network for Lightweight Image Super-Resolution.” arXiv arXiv, 2020.
- [133] C. Wang *et al.*, “Transform Domain Based Medical Image Super-resolution via Deep Multi-scale Network.” in *ICASSP 2019 - 2019 IEEE International Conference on Acoustics, Speech and Signal Processing (ICASSP)*, Brighton, United Kingdom: IEEE, May 2019, pp. 2387–2391.
- [134] K. Shen *et al.*, “Physics-driven deep learning photoacoustic tomography,” *Fundamental Research*, p. S2667325824003583, Sep. 2024.
- [135] F. Zhu and W. Liu, “A novel medical image fusion method based on multi-scale shearing rolling weighted guided image filter,” *MBE*, vol. 20, no. 8, pp. 15374–15406, 2023.
- [136] J. Ma *et al.*, “GANMcC: A Generative Adversarial Network With Multiclassification Constraints for Infrared and Visible Image Fusion,” *IEEE Trans. Instrum. Meas.*, vol. 70, pp. 1–14, 2021.
- [137] N. Nyayapathi *et al.*, “Dual-modal photoacoustic and ultrasound imaging: from preclinical to clinical applications,” *Front. Photon.*, vol. 5, p. 1359784, Feb. 2024.
- [138] Y. Notsuka *et al.*, “Improvement of spatial resolution in photoacoustic microscopy using transmissive adaptive optics with a low-frequency ultrasound transducer,” *Opt. Express*, vol. 30, no. 2, p. 2933, Jan. 2022.
- [139] S. K. Biswas *et al.*, “A Method for Delineation of Bone Surfaces in Photoacoustic Computed Tomography of the Finger,” *Ultrason Imaging*, vol. 38, no. 1, pp. 63–76, Jan. 2016.
- [140] T. D. Le, S.-Y. Kwon, and C. Lee, “Segmentation and Quantitative Analysis of Photoacoustic Imaging: A Review,” *Photonics*, vol. 9, no. 3, p. 176, Mar. 2022.